Fluent speech: neural basis of sensorimotor plasticity in developmental stuttering

Alexandra Korzeczek[1,#,*], Annika Primaßin[1,2#], Alexander Wolff von Gudenberg[3], Peter Dechent[4], Walter Paulus[1], Martin Sommer[1], and Nicole E. Neef[1,*]

[1]Department of Clinical Neurophysiology, Georg-August-University, Göttingen, Germany

[2]Present address: FH Münster University of Applied Sciences, Münster School of Health (MSH), Münster, Germany

[3]Institut der Kasseler Stottertherapie, Bad Emstal, Germany

[4]MR Research in Neurology and Psychiatry, Department of Cognitive Neurology, Georg-August-University, Göttingen, Germany

[#]**These authors contributed equally**

*C**orrespondence:**

Alexandra Korzeczek
Department of Clinical Neurophysiology
University Medical Center
Robert-Koch-Straße 40
37075 Göttingen, Germany
Email: alexandra.korzeczek@med.uni-goettingen.de

Nicole E. Neef
Department of Clinical Neurophysiology
University Medical Center
Robert-Koch-Straße 40
37075 Göttingen, Germany
Email: nneef@gwdg.de

Running title: Sensorimotor plasticity in stuttering

Abstract

Developmental stuttering is a fluency disorder with anomalies in the neural speech motor system. Fluent speech requires multifunctional network formations. Currently, it is unclear which functional domain is targeted by speech fluency interventions. Here, we tested the impact of fluency-shaping on resting-state fMRI connectivity of the speech planning, articulatory convergence, sensorimotor integration, and inhibitory control network. Furthermore, we examined white matter metrics of major speech tracts. Improved fluency was accompanied by an increased synchronization within the sensorimotor integration network. Specifically, two connections were strengthened, left laryngeal motor cortex and right superior temporal gyrus showed increased connectivity with the left inferior frontal gyrus. The integration of the command-to-execution and auditory-motor pathway was strengthened. Since we investigated task-free brain activity, we assume that our findings are not biased to network activity involved in compensation. No alterations were found within white matter microstructure. But, brain-behavior relationships changed. We found a heightened negative correlation between stuttering severity and fractional anisotropy in the superior longitudinal fasciculus, and a heightened positive correlation between the psycho-social impact of stuttering and fractional anisotropy in the right frontal aslant tract. Taken together, structural and functional connectivity of the sensorimotor integration and inhibitory control network shape speech motor learning.

Keywords

neural speech networks, stuttering intervention, sensorimotor integration, MRI, neuroplasticity, inferior frontal gyrus

Introduction

Fluent speech requires a complex interplay of multiple neuronal networks. These networks incorporate speech planning[1,2], sensorimotor integration[3–6], articulatory convergence[7–9], and the inhibition of competitive processes[10,11]. In developmental stuttering, a heritable speech fluency disorder[12] of unknown origin[13,14], neuroimaging studies indicate aberrant brain activity and connectivity, in particular in brain structures that convey the abovementioned functions (for an overview see e.g.[15]. However, especially in adults who experienced lifelong stuttering it is difficult to differentiate core neural deficits from stuttering-induced neural signatures, respectively, therapy-induced neuroplasticity from compensatory network activity. Thus, our understanding of neurophysiological mechanistic principles of stuttering and its neural remediation remains limited.

Neuroimaging studies provide much of the early evidence implicating particular brain regions in developmental stuttering[8]. Quantitative meta-analyses link stuttering to reduced left fronto-parieto-temporal speech network activity while greater speech fluency of affected individuals is associated with boosted co-activations of homologue right fronto-parietotemporal areas[16–19]. In addition to irregular activity patterns, further imaging findings indicate white matter deficits[20–24] in the dorsal language pathway[25,26], the frontal motor pathway[26,27] and interhemispheric connections between the sensorimotor cortices[19]. Movement control engages the basal ganglia and the cerebellum, further crucial brain regions that show abnormal activity and connectivity in adults with persistent developmental stuttering[21,24,28,29]. Taken together, findings give rise to different theories of stuttering, which is seen as a problem of sensorimotor integration and timing, either caused by a basal ganglia dysfunction or caused by a disconnection of cortical speech regions (Civier et al., 2013).

Speech production in stuttering is characterized by sound and syllable repetitions, sound prolongations and speech blocks, which can be accompanied by physical concomitants such as facial grimacing, head or limb movements. One common approach to overcome these characteristic motor signs of stuttering is fluency shaping, a speech restructuring method that require individuals who stutter to learn a changed speech pattern. In the current study, this learning process was embedded

in an intensive two-week on-site intervention and a one-year stand-alone speech training that required computer-assisted daily practice[30]. It is well established that extensive sensorimotor learning induces neuroplasticity[31]. Here it is not the question whether the extensive speech training shapes speech related brain structures and dynamics, but which concrete networks are addressed.

One suitable approach to scrutinizing learning-induced neuroplasticity is the use of resting-state functional magnetic resonance imaging (rs-MRI). On the one hand, rs-fMRI is free from confounds of task performance, particularly in participants who may present symptoms such as physical concomitants during speaking. Thus, task-free brain activity assesses changes in brain dynamics that are not biased by differences in how a task is performed in pre-learning versus post-learning condition[32]. On the other hand, it is widely assumed that spontaneous ongoing global activity of the brain at rest is highly structured, closely relates to underlying anatomical connectivity and reflects local neuronal dynamics, signal transmission delay and genuine noise[33]. It has been shown that even under resting-state condition brain areas show activity changes with learning and correlated activity increases between learning related areas[6,32,34].

Until today task-free brain activity has been studied twice to test stuttering intervention induced neuroplasticity[35,36]. In the earlier study, an independent component analysis was used to identify the spatial map of the speech-language network at an individual level. Selected speech-language components were fed into group-wise random effects two sample *t* tests resulting in an intervention-induced decrease of resting state connectivity in the left declive and vermis area of the cerebellum in the intervention group, but not among the other groups of the study, i.e. fluent controls and individuals who stutter with no intervention. This change in rs-fMRI connectivity was correlated with the intervention-induced change in stuttering frequency[35]. The analysis approach is uncommon and an attempt to replicate this finding was not successful[36]. Other studies that tested stuttering intervention induced neuroplasticity used speech tasks such as overt single word reading[36], overt sentence reading[28,37–41], and picture naming[42]. Fluency shaping, the stuttering intervention also tested in the current study, induced a re-lateralization of speech-induced brain activity towards the

left hemisphere[38,40] possibly due to an improvement of auditory-motor mapping[41] and a restructuring of prosody production[43]. Across stuttering intervention studies, induced plasticity mainly involved the left inferior frontal gyrus[36,40,41,43]. Task-activity however, encompass all components of fluent speech production such as speech planning, articulatory convergence, sensorimotor integration, and the inhibition of non-desirable movements as well as different cognitive strategies to perform the task.

Here, we use a longitudinal approach to examine stuttering-intervention-induced improvement in speech fluency and related neurofunctional reorganization. We analysed rs-fMRI data acquired before and 11 months after the computer-assisted speech-restructuring intervention[30]. We quantify the synchronicity of spontaneous low frequency fluctuations to characterize the connectivity between functionally related brain hubs of speech planning[44], articulatory convergence[9], speech-related sensorimotor integration[6], and speech motor inhibitory control[11,44]. We test time-dependent changes in rs-fMRI connectivity[45] in persons who stutter who participated in the intensive intervention (PDS+), and we control for the specificity by studying two control groups, i.e. patients with developmental stuttering not taking part in any stuttering intervention (PDS-) and healthy controls (HC). Furthermore, we test whether intensive stuttering intervention induces changes in white matter tissue properties within two tracts thought to carry signals critical for speech fluency [27,46], the superior longitudinal fasciculus (SLF), the frontal aslant tract (FAT). In addition, as a control we examine a tract crucial for current rs-fMRI findings. Finally, we explore correlations between neuroplasticity and behavior.

Methods

Participants

Current data have been collected during a dissertation project[47] that evaluated the long-term effects of an intensive stuttering intervention on white matte integrity and task-related brain activity. Seventy-six right-handed, monolingual speakers of German participated on a voluntary basis in the

current controlled trial. Exclusion criteria were any speech or language disorder other than developmental stuttering, neurological impairment, drug abuse, or medications that act on the CNS. None of the PDS- took part in any stuttering therapy during the entire study period. For analysis, we excluded the data of three participants who in spite of being informed participated in a different stuttering intervention, of four participants with missing behavioral or rs-fMRI data and of one participant with rs-fMRI motion artifacts. Thus, rs-fMRI data analysis comprised 22 PDS+ (2 females, mean age 25.6 ± 11.7), 18 PDS- (2 females, mean age 34.8 ± 7.0), and 28 HC (4 females, mean age 25.1 ± 7.4). The groups were matched with regard to sex and handedness[48]. PDS- were older and had a higher education score than participants in the two other groups (see Table 1). Since education correlated with age, $r = 0.483$, $p < 0.001$, only age was included as a covariate in the statistical analyses. Speech fluency (Stuttering severity index, SSI-4)[49] of all participants was assessed prior to each MRI session. Stuttering severity was similar in stuttering groups, HC showed lower SSI-4 scores due to their fluent speech (Table 1). In addition, a self-assessment of the psycho-social impact of stuttering (Overall Assessment of the Speaker's Experience of Stuttering, OASES)[50] indicated that PDS+ suffered more from stuttering than PDS-, which might possibly relate to age and age-related requirements of living.

Table 1 Demographic information of participants

	PDS+	**PDS-**	**HC**	**Test-statistics (*df*)**	**two-sided *p*-value**
n	22	18	28		
Age, years	25.6 ± 11.7	34.8 ± 7.0*	25.1 ± 7.4	7.58 (2, 65)[i]	0.001
Sex ratio	20:2	16:2	24:4	–[ii]	0.89
Education[a]	2 (1.0)[#]	6 (3.0)	3 (2.8)	27.49 (12)[iii]	< 0.001

Handedness	91 (12)	91 (33)	100 (33)	0.04 (2,68) [iii]	0.98
SSI-4 at T1	25 (14.3) [#]	14 (11.3)	–	2.56 [iv]	0.010
SSI-4 at T2	9 (10.5)	12.5 (11.0)	–	-1.31 [iv]	0.194
OASES at T1	3.0 (0.6) [#]	2.0 (0.4)	–	4.70 [iv]	< 0.001
OASES at T2	1.9 (0.5)	2.0 (0.5)	–	-0.65 [iv]	0.516
Onset, years	4.8 ± 3.0	5.0 ± 3.6	–	0.22 [iv]	0.839
Interval, months	11.6 ± 1.0	11.6 ± 1.4	11.4 ± 0.8	0.95 (2) [iii]	0.623

*Interval/ratio -scaled variables are presented as mean ± standard deviation. Ordinal-scaled variables are presented as median (interquartile range). *significantly different from both other groups in post hoc comparisons (p < 0.001),[#]significantly different from stuttering controls (p < 0.001),[i]one-way independent ANOVA,[ii]Fisher's exact test,[iii]Kruskal-Wallis test,[iv]Mann-Whitney test,[a]1 = still attending school, 2 = school, 3 = high school, 4 = <2years college, 5 = 2 years of college, 6 = 4 years of college, 7 = postgraduate*

The ethical review board of the University Medical Center Göttingen, Georg August University Göttingen, Germany, approved the study, and all participants provided written informed consent, according to the Declaration of Helsinki, before participation.

All participants participated in two MRI sessions (T1 and T2) separated by 10 to 15 months. The scanning interval was similar between groups (Table 1). PDS+ were scanned pre- (T1) and post-intervention (T2).

Intensive stuttering intervention and follow-up care

PDS+ took part in the Kasseler Stotter Therapie[30] that incorporates fluency shaping with computer-assisted biofeedback during a two-week on-site and a one-year follow-up treatment. Fluency shaping reconstructs patterns of vocalization, articulation and respiration, resulting in prolonged speech, soft voice onsets of initial phonemes and a smooth transition between sounds. The follow-up period consists of two refresher courses at the therapy center, one month and ten months after the intensive training, respectively, as well as a daily biofeedback-assisted practice of the new speech patterns. Daily practice intensity was monitored by the computer.

Assessment and statistical analysis of behavioral data

Changes in speech fluency were assessed by two experienced speech and language pathologists (one of them was AP) with the Stuttering Severity Index (SSI-4). Each speech sample comprised 488 to 500 syllables. To ensure interrater reliability, both raters analyzed nine randomly chosen participants, three from each group. Reliability estimates, as assessed with Krippendorff's Alpha, ranged between 0.84 and 0.96, indicating a good interrater reliability. The participants' experience with stuttering was assessed with the German version of the OASES[50]. We assessed behavioral changes as a change of the total scores of the SSI-4 and OASES between T1 and T2 using R (version 3.5.3). We ran robust mixed ANOVAs on trimmed means with group as between-factor and time as within-factor using the package WSR (version 0.37). Post hoc we applied Wilcoxon signed-rank tests.

Definition of four speech-related semi-discrete brain networks

Fluent speech production engages large-scale brain networks conveying emotional, linguistic, cognitive, sensory, and motor functions. Among these processes, a dysfunctional speech planning, articulatory convergence, sensorimotor integration or motor inhibition most likely cause the primary motor signs of stuttering, which are sound and syllable repetitions, sound prolongations and speech

blocks. Here, we distinguished four semi-discrete brain networks consisting of brain regions that are recruited for any of these functions (Fig. 1).

Selected brain region of dysfunctional *speech planning* were derived from an earlier fMRI study of our lab investigating imaginary of speaking compared to humming[44] (Fig. 1A). *Articulatory convergence* seeds originated from a combined ALE meta-analyses[9] on brain imaging studies of simple articulatory movements of jaw, larynx, lips, tongue, and respiratory system (Fig. 1B). Speech-related *sensorimotor integration* seeds were derived from a listen and repeat localizer task in a brain imaging study of sensorimotor plasticity in speech motor adaptation[6] (Fig. 1C). *Motor inhibition* seeds that involve common areas of inference resolution, action withholding, and action cancellation were derived from a meta-analysis[51]. We added the subthalamic nucleus seed to the inhibition network to account for the dedicated involvement of this structure in response inhibition[52] (Fig. 1D). We created spherical seeds with a radius of 6 mm for all ROIs. Coordinates for brain hubs involved in speech-related sensorimotor integration can be found in Table 2. Seeds for the remaining three networks are listed in Supplementary Table 1. Seed ROIs did not overlap.

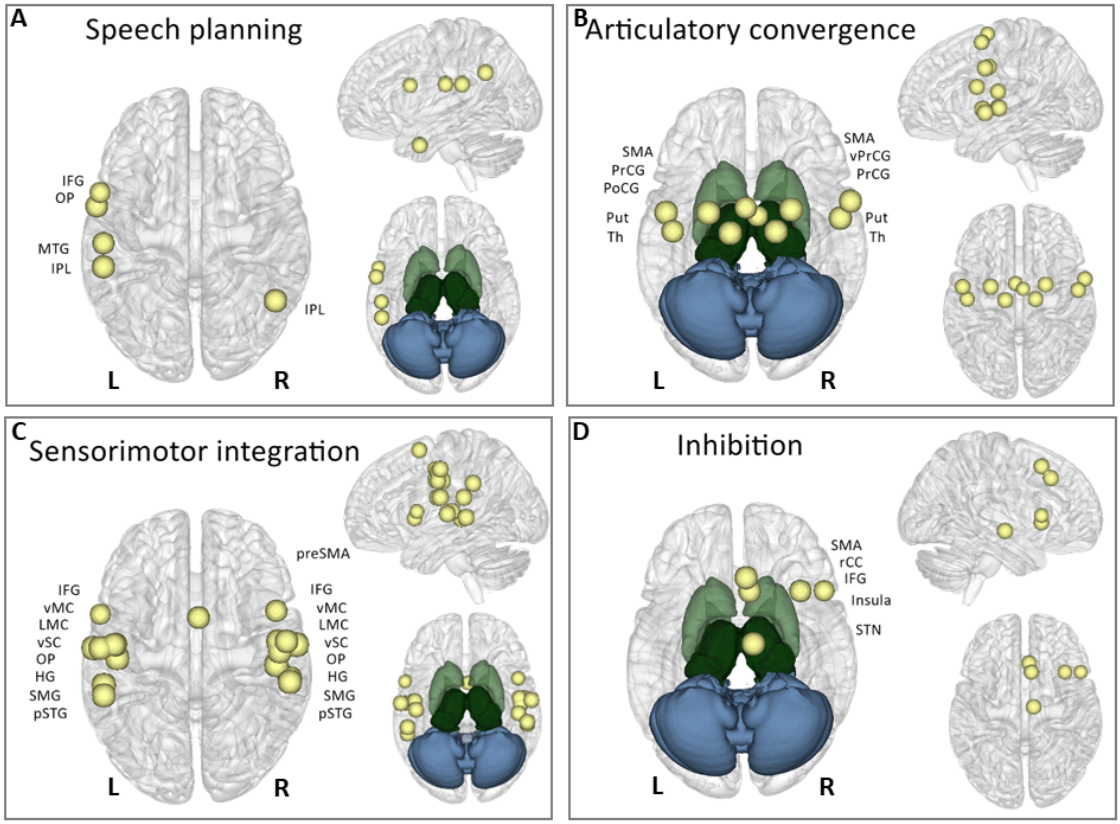

Figure 1 ROI-to-ROI resting state fMRI analysis was conducted in four semi-discrete functional networks. *Spheres with a diameter of 6 mm served as regions of interest and are displayed on rendered surfaces of the MNI standard brain. Intervention effects were tested for speech planning (A), articulatory convergence (B), sensorimotor integration (C), and motor inhibition (D). HG = Heschl' s gyrus, primary auditory cortex; IPL = inferior parietal lobe; IFG = inferior fronatal gyrus, Broca's region; LMC = laryngeal motor cortex; MTG = middle temporal gyrus; OP = parietal operculum; PoCG = postcentral gyrus; PrCG = precentral gyrus; preSMA = pre-supplementary motor area; pSTG = posterior superior temporal gyrus; Put = putamen; rCC = rostral cingulate zone; SMA = supplementary motor area; SMG = supramarginal gyrus; STN = subthalamic nucleus; Th = thalamus; vMC = ventral primary motor cortex; vPrCG = ventral precentral gyrus; vSC = ventral primary somatosensory cortex.*

Table 2 Brain hubs of speech-related sensorimotor integration

Brain hub – anatomical label	ROI Label	X	Y	Z

Inferior frontal gyrus, posterior-ventral, Broca's region	L IFG	-56	8	8
	R IFG	48	10	2
Pre-supplementary motor area	R preSMA	2	6	60
Ventral primary motor cortex	L vMC	-48	-10	42
	R vMC	54	-8	44
Laryngeal motor cortex	L LMC	-47	-10	34
	R LMC	49	-8	35
Ventral primary somatosensory cortex	L vSC	-56	-12	44
	R vSC	50	-14	34
Parietal Operculum, secondary somatosensory cortex	L OP	-60	-12	20
	R OP	60	-10	20
Supramarginal gyrus	L SMG	-54	-40	32
	R SMG	56	-32	2
Heschl's gyrus, primary auditory cortex	L HG	-46	-18	6
	R HG	48	-22	8
Posterior superior temporal gyrus	L pSTG	-54	-34	3
	R pSTG	56	-30	3

All coordinates refer to MNI-space. L = left, R = right. Coordinates were derived from a listen and repeat speech task[6].

MRI acquisition protocol

MRI data were acquired in a 3 Tesla Siemens Magnetom Tim Trio scanner (Erlangen, Germany) using an eight-channel phased-array head coil at the University Medical Center Göttingen, Germany. Sagittal T1 weighted structural data were acquired with a 3D turbo fast low angle shot (FLASH) sequence (TR = 2250ms, TE = 3.26ms, TI = 900ms, flip angle = 9°, 256mm FoV, 7/8 Fourier phase encoding) as whole-brain anatomical reference data at a spatial resolution of $1 \times 1 \times 1$ mm³ voxel

size (256 × 256 matrix). For resting-state fMRI a gradient-echo echo planar imaging (EPI) sequence (TR = 1800ms, TE = 30ms, flip angle = 70°, parallel acquisition factor 2, 192 mm FoV, 33 slices, 194 volumes) was used with isotropic voxels at 3 $(mm)^3$ and a 64 x 64 acquisition matrix. We acquired two six-minute rs-fMRI time series at T1 and at T2, respectively, while participants fixated a cross in an open eyes condition. Due to different head sizes the rs-fMRI data did not fully cover the cerebellum in some participants. Therefore, the cerebellum was excluded in further rs-fMRI analyses. Diffusion-weighted MRI was performed using a spin-echo EPI sequence (TR = 10100 ms, TE = 93 ms, parallel acquisition factor 2, 6/8 Fourier phase encoding**,** 243mm FoV, acquisition matrix: 128 × 128, 74 slices, voxel size 1.9 x 1.9 x 1.9 mm^3) acquiring 64 image volumes with diffusion weighting along 64 diffusion directions (b = 1000 s/mm^2) and one reference image without diffusion weighting. Participants lay in supine position in the scanner and wore headphones for noise protection, and MR-compatible LCD goggles (VisuaStim XGA, Resonance Technology Inc., Northridge, CA, USA).

Rs-fMRI data processing and analysis

Structural and functional MRI data were preprocessed and analyzed with CONN functional connectivity toolbox version 18b[53]. The toolbox is based on Matlab and Statistical Parametric Mapping (SPM). The standard preprocessing pipeline of CONN was used: Structural data were centered to (0,0,0) coordinates, segmented and normalized to MNI-space. Functional data were realigned and centered to (0,0,0) coordinates, slice-timing corrected, checked for outliers using 95th percentiles settings[54,55], direct segmented and normalized to MNI-space. Finally, functional images were smoothed with a Gaussian kernel of 8mm FWHM (full-width half-maximum). After these preprocessing steps, functional data were corrected for white matter and cerebro-spinal fluid signals, motion and scrubbing as well as effects of measurements using linear regression. Following regression, a 0.009 - 0.08 HZ bandpass filter was applied.

To test for an intervention-induced neuroplasticity, we calculated Fisher-transformed correlation coefficients off bivariate ROI-to-ROI correlations with hemodynamic response function weighting for each of the four predefined semi-discrete speech-related networks (Fig. 1). Second-level analyses comprised four global (3×2×17) mixed model ANCOVAs with Group as between–subjects factor, Time and ROIs as within-subjects factors and age with grand mean centering as covariate. Multiple comparison correction was performed with a connection threshold at seed level *p-FDR* < 0.05 (two-sided) and a seed-level permutation analysis threshold based on a Network Based Statistics by intensity approach[12] with *p-FDR* < 0.05. In case of a significant Group x Time interaction, we run subsequent post hoc analyses to distinguish group effects in those connectivity changes. Effect sizes are reported with beta values which represent average functional connectivity (Fisher-transformed correlation coefficients) among the tested contrasts.

Diffusion-weighted imaging data processing and analyses

Diffusion data were preprocessed with tools from the FMRIB Software Library, (FSL 6.0 on a Linux machine with Ubuntu LTS 18.04, http://www.fmrbi.ox.ac.uk/fsl/). Fiber tracking was carried out on aligned, distortion corrected, concatenated datasets that were collected across T1 and T2 for each subject to ensure that estimates of diffusivity and diffusion anisotropy across sessions were mapped to the same anatomical location for each subject. White matter tracts were identified with the Automated Fiber Quantification software implemented in python (pyAFQ, https://github.com/yeatmanlab/pyAFQ)[56]. Within pyAFQ individual b0 images were aligned with the native anatomy via an affine registration and warped to the FSL_HCP1065_FA_1mm template via a nonlinear registration. Inverted warp maps were used to register waypoint masks and exclusion masks with individual b0 images. A whole brain tractogram was generated in the native space of each participant with a deterministic tracking algorithm with a fourth-order Runge–Kutta path integration method (1 mm fixed step size, 8 seed points per voxel, FA threshold 0.2 and 30 °, minimum streamline length set to 10 mm). We segmented the superior longitudinal fasciculus (SLF), the frontal

aslant tract (FAT) and the tract connecting LMC and IFG in the left and right hemisphere, respectively. For tract segmentation the whole brain tractogram was filtered, first with a tract-specific probability map, second with waypoint and exclusion masks and third with cortical endpoint masks. A detailed description is provided in the Supplementary Material. Visual inspection of the tracts and manual cleaning was performed via TrackVis 0.6.1 (http://trackvis.org/). Not all tracks could be segmented in all participants as reported in Supplemental Tables 7-11.

Finally, we fitted the diffusion kurtosis model, implemented in DIPY (https://dipy.org/)[57], to the diffusion data separately for each session and projected the fractional anisotropy (FA), mean diffusivity (MD), radial diffusivity (RD) and axial diffusivity (AD) onto the segmented fiber tracts generated by pyAFQ. Therefore, selected tracts were sampled into 100 evenly spaced nodes, spanning the two termination points. To determine changes in diffusion properties we built the difference wave between T2 and T1 and averaged the values of the inner 60 nodes. This procedure was adopted from a report of rapid white matter changes after an intensive reading intervention[58]. The change in diffusivity and diffusion anisotropy was tested against zero separately for each tract and each group and Bonferroni-corrected to account for multiple testing.

Correlation analyses

Finally, Pearson correlations were calculated in MATLAB (R2018b) to test brain behavior relationships for rs-fMRI and dMRI metrics.

Data availability statement

The data that support the findings of this study are available from the corresponding author upon reasonable request.

Results

Computer-assisted intensive intervention improved speech fluency and well-being

A reduction in the total scores of the Stuttering Severity Index (SSI-4) and the Overall Assessment of the Speaker's Experience of Stuttering (OAESES) as seen here indicates a positive outcome of stuttering intervention. The robust ANOVA for stuttering severity revealed a significant interaction of Group by Time, $Q = 24.44$, $p < 0.001$, an effect of Group $Q = 48.38$, $p < 0.001$, and an effect of Time $Q = 50.99$, $p < 0.001$. Post hoc tests revealed that in the intervention group, stuttering severity decreased from T1 to T2, $V = 253$, $p < 0.001$, $r = -0.87$ (Fig. 2A). In contrast, in the non-intervention groups the SSI-4 scores remained unchanged with $V = 63$, $p = 0.81$, $r = -0.06$ for PDS- and $V = 58.5$, $p = 0.38$, $r = -0.17$ for HC. Similarly, the robust ANOVA for the speaker's experience of stuttering revealed a significant interaction of Group by Time, $Q = 66.73$, $p < 0.001$, an effect of Group $Q = 20.39$, $p < 0.001$ and an effect of time $Q = 74.17$, $p < 0.001$. Post hoc tests revealed that a decrease in the OASES-scores between T1 and T2 emerged only in PDS+, $V = 253$, $p < 0.001$, $r = -0.87$ (Fig. 2B). PDS- yielded no changes in their experience with stuttering, $V = 110.5$, $p = 0.29$, $r = -0.25$. Behavioral outcome measures are summarized in Supplementary Table 6.

Intervention strengthened a dedicated speech motor learning connection

Only one of the four global mixed model ANCOVAs revealed significant results. When seeds of the sensorimotor integration network were inserted in the analysis, the left IFG showed a Group × Time × Target interaction with $X(28) = 48.57$, Intensity = 21.57, $p = 0.005$. Specifically, the factors Group and Time had an effect on the connectivity between left IFG and left LMC, beta = 0.12, $F(2,64) = 8.71$, $p = 0.007$, the left IFG and the left SMG, beta = 0.24, $F(2,64) = 7.4$, $p = 0.01$, and the left IFG and the right pSTG, beta = 0.13, $F(2,64) = 5.47$, $p = 0.034$ (Figure 2A, upper panel). There were no main effects of Group or Time. Results of connection-wise, post hoc two-sample t-tests controlling for age are listed in Table 3. For the left IFG-to-left LMC connection the analyses revealed a higher change in

connectivity for PDS+ when compared to HC and when compared to PDS-. For the left IFG-to-right pSTG connection a higher change in connectivity was evident in PDS+ compared to HC and showed a trend when inserting PDS+ and PDS-. For the left IFG-to-SMG connection the analyses revealed a higher change in connectivity for PDS- compared to HC and showed a trend for PDS+ compared to HC (Supplementary Figure 2). A final post-hoc 2 × 17 ANCOVA with an analysis-level correction for multiple comparison of seeds and targets confirmed the influence of Time on the synchronicity between left IFG and left LMC in PDS+ with beta = 0.1, $T(20) = 5.47$, $p = 0.003$ (Figure 2A, lower panel).

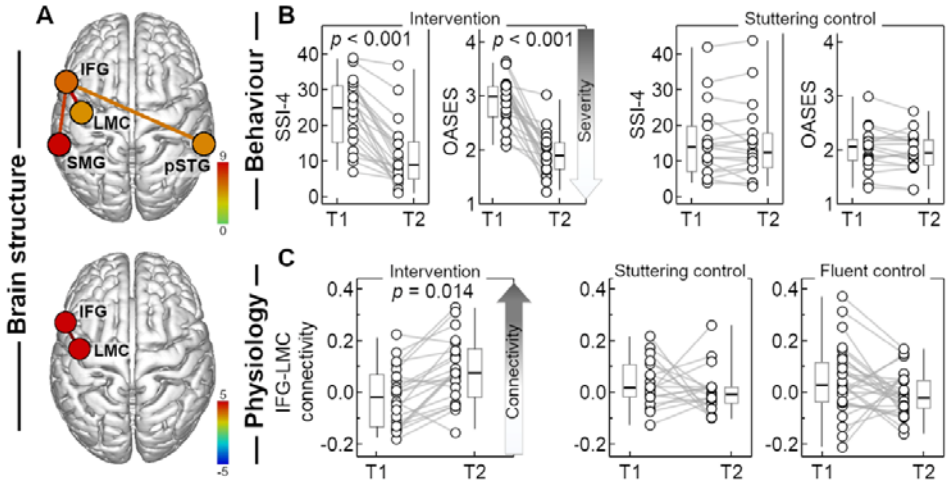

Figure 2 Intensive computer-assisted intervention reduced stuttering and strengthened IFG-to-LMC rs-connectivity within the sensorimotor integration network. *On the behavioral level (upper panel) stuttering severity decreased between pre- (T1) and 11-months post-intervention (T2) as shown by the reduced SSI-4 scores, scaling from 0 (none) to 46 (very severe), and the reduced OASES-scores, scaling from 1 (mild) to 5 (severe) in the intervention group (PDS+). In contrast, stuttering controls showed no changes of stuttering severity. On the physiological level (lower panel) ROI-to-ROI functional connectivity analysis revealed a boosted correlation within the speech-related sensorimotor integration network in the intervention group. Left IFG-LMC-correlation was increased as shown by comparison of beta estimates between pre- (T1) and one-year post-intervention (T2). The two control groups, stuttering control and fluent controls, showed no changes of connection strength. IFG = inferior frontal gyrus; LMC = laryngeal motor cortex; pSTG = posterior superior*

temporal gyrus; SMG = supramarginal gyrus. (D) Illustration of IFG and LMC locations on the rendered surface of the human brain. The result is significant at p < 0.05, analysis-level false discovery rate (FDR) corrected. IFG = inferior frontal gyrus pars opercularis; LMC = laryngeal motor cortex; OASES = Overall Assessment of the Speaker's Experience of Stuttering; ROI = region of interest; SSI = Stuttering Severity Index.

Table 3 Post hoc analyses

Seed - target region	Analysis	*Beta*	Test value(*DF*)	*p*
left IFG – LMC	PDS+ vs. HC	0.14	3.77 *(46)*	< 0.001
	PDS+ vs. PDS-	0.12	2.47 (36)	0.018
	PDS- vs. HC	0.024	0.41 (42)	0.683
left IFG – SMG	PDS+ vs. HC	0.08	1.8 (46)	0.079
	PDS+ vs. PDS-	-0.05	-0.81 (36)	0.426
	PDS- vs. HC	0.13	2.1 (42)	0.042
left IFG – right pSTG	PDS+ vs. HC	0.14	2.89 (46)	0.006
	PDS+ vs. PDS-	0.11	1.85 (36)	0.073
	PDS- vs. HC	0.035	0.51 (42)	0.609

No correlation between rs-connectivity and improvement after stuttering intervention

Neither the change in speech fluency (SSI-4) nor the experience of stuttering (OASES) correlated with rs-connectivity, all $p > 0.05$.

No changes in diffusion properties due to intervention

None of the three white matter tracts showed a significant change in any of the diffusion properties, FA, MD, RD or AD in PDS+. PWS- showed a change of FA in the left IFG-to-LMC tract ($t(18) = -2.86$, $p = 0.048$) and HC showed a change of FA in the left SLF ($t(26) = -4.33$, $p = 0.001$) together with a change of RD ($t(26) = 2.71$, $p = 0.048$), and a change of FA in the right SLF ($t(24) = -3.08$, $p = 0.021$). HC

showed in addition a change of AD in the right IFG-to-LMC tract ($t(26)= -3.33$, $p = 0.012$). Figure 3 illustrates the segmented tracts of the left hemisphere and its FA profiles together with the magnitude of change in FA and MD. Tract specific group averages, standard deviations, *t*-values and *p*-values for all diffusion metrics are listed in Supplemental Table 7.

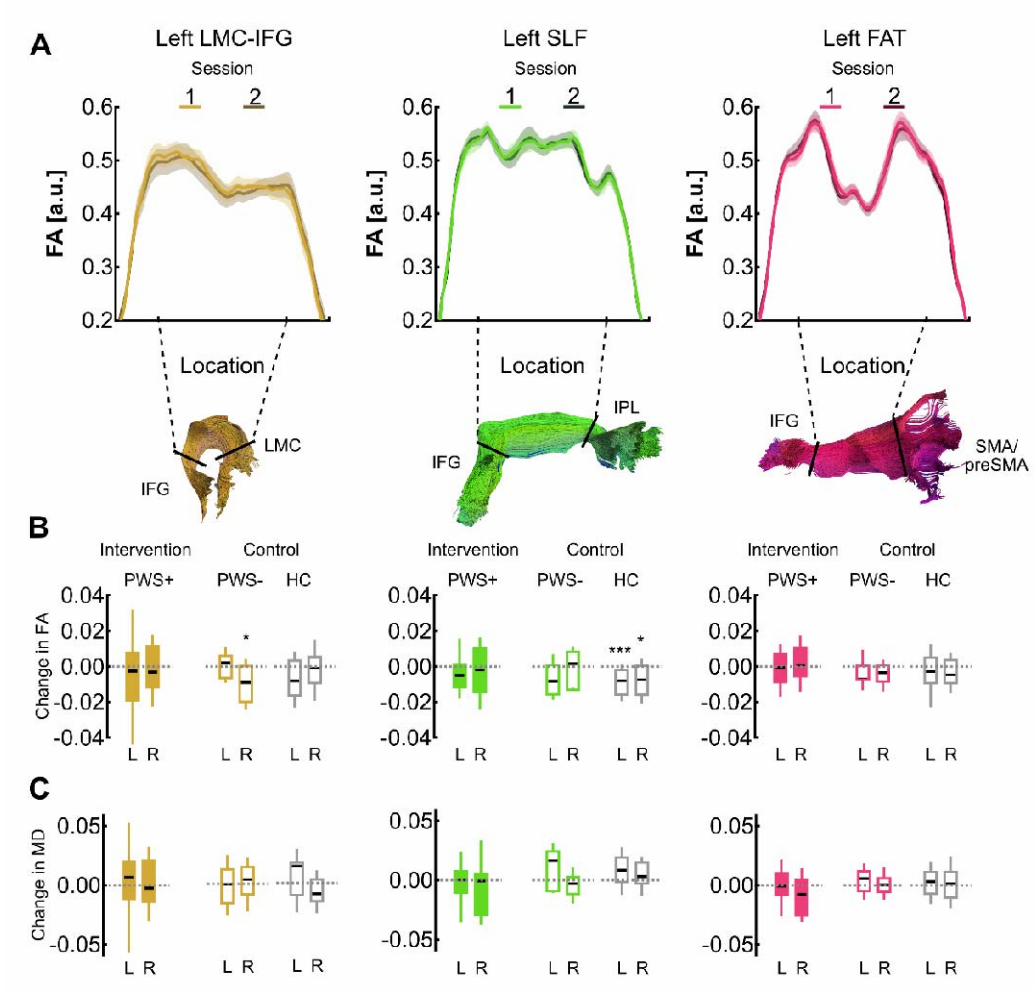

Figure 3 No intervention-related white matter changes in three speech motor tracts. *(A) Fractional anisotropy, FA, was mapped onto 100 evenly spaced points connecting cortical speech regions. Each curve represents the group average FA across participants of the intervention group (PWS+, n = 22) for the white matter connecting the left laryngeal motor cortex (LMC) and the left inferior frontal gyrus (IFG, brown), the left superior longitudinal fasciculus (SLF, green), and the left frontal aslant tract (FAT, red). Pale colors show pre-intervention FA (Session 1) and dark colors show FA after ~11 months of intervention (Session 2). Shaded areas give ±1*

*standard error of the mean. Each tract was clipped prior to analysis as shown with black boundary lines in corresponding tract renderings. To avoid pruning effects that occur at endpoints of the tract, only the middle 60% of each tract was considered in the analyses of FA (B) and mean diffusivity, MD (C). Box plots illustrate the magnitude of change observed relative to Session 1 for the left (L) and right (R) hemisphere for the intervention group (filled boxes) and the two control groups (stuttering without intervention, PWS-; and fluent speakers without intervention, HC; unfilled boxes). Whiskers indicate ± one standard deviation. Asterisks indicate a significant increase in FA (B) or decrease in MD (C) at a Bonferroni-corrected *p < 0.05 and ***p < 0.001.*

Relieve from stuttering relates to white matter integrity of SLF and FAT

We calculated point-wise Pearson correlations between diffusion metrics projected to the SLF, FAT and LMC-to-IFG connection and the motor signs of stuttering measured with SSI-4. At T2, SSI-4 scores of PWS+ correlated negatively with FA values projected to the posterior part of the left SLF. Bootstrapping with a boot size of 100000 revealed significant point-wise correlations at $p < 0.005$ with a cluster-size significance at $p < 0.01$ (Figure 4A-B). Thus, after intervention, mild stuttering was related to higher FA values, while severe stuttering was related to lower FA values in the left SLF. At T1, correlations in the same SLF region did not survive correction for multiple comparisons (Figure 4A, C). We calculated a *z*-score of the difference between the correlation coefficients. With a difference score of $z = 1.79$ and a two-tailed $p = 0.073$, the correlations between FA at T2 and SSI-4 trended to be higher than the correlation between FA at T1 and SSI-4. No other correlation between SSI-4 and white matter characteristics reached statistical significance.

The psycho-social impact of stuttering, as measured with the OASES, was positively correlated with the middle portion of the right FAT (Figure 4B, D). Thus, after intervention mild suffering from stuttering was related to lower FA values, while severe suffering from stuttering was related to higher FA values in the right FAT. Bootstrapping with a boot size of 100000 revealed significant point-wise correlations at $p < 0.005$ with a cluster-size significance at $p < 0.02$. With a difference score of $z = -2.89$ and a two-tailed $p = 0.004$, the correlation between FA at T2 and OASES was significantly

higher than the correlation between FA at T1 and OASES. No other correlation between OASES and white matter characteristics reached statistical significance.

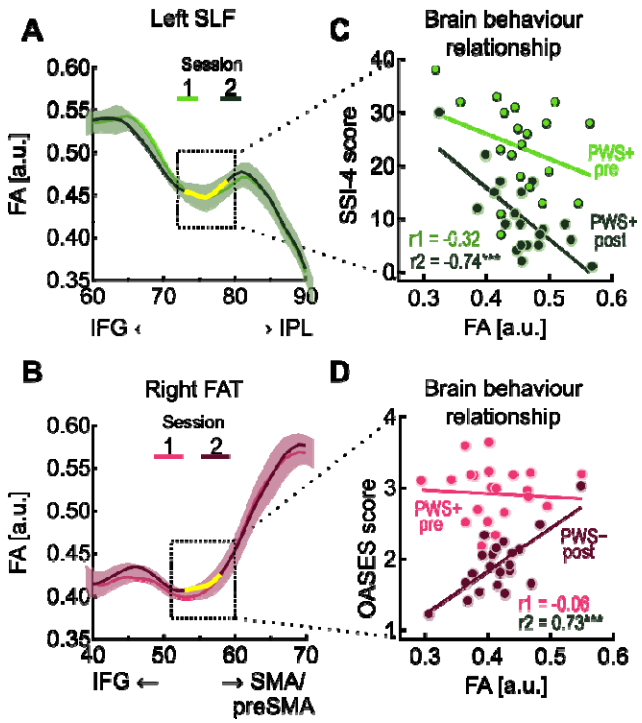

Figure 4 Brain behavior relationship changed with intervention. *Each curve represents the group average FA across participants of the intervention group (PWS+) from the posterior part of the left superior longitudinal fasciculus (SLF, A), and from the medium part of the right frontal aslant tract (FAT, B). Pale colors show pre-intervention FA (Session 1) and dark colors show post intervention FA (Session 2). Shaded areas give ± 1 standard error of the mean. (C) Stuttering severity (SSI-4 scores) is plotted against FA values averaged across tract points 73 to 81 framed with a dotted square in A. The Pearson correlation was significant at ***p < 0.001. Bootstrapping with a boot size of 100000 revealed significant point-wise correlations at p < 0.005 with a cluster-size significance at p < 0.01 highlighted with yellow in A. (D) Experience of stuttering (OASES scores) is plotted against FA values averaged across tract points 52 to 61 framed with a dotted square in B. The Pearson correlation was significant at ***p < 0.001. Bootstrapping with a boot size of 100000 revealed significant point-wise correlations at p < 0.005 with a cluster-size significance at p < 0.02 highlighted with yellow in B.*

Discussion

A one-year technology-based speech-restructuring training sustainably facilitated speech fluency of patients with developmental stuttering. As a neural correlate we found a strengthened synchronization of the posterior-ventral IFG pars opercularis with the laryngeal motor cortex within the sensorimotor integration network as evidenced by resting-state functional brain activity. Hence, here we show for the first time that a computer-assisted biofeedback-based, intensive speech training program induced functionally specific, focal and long-lasting changes in task-free brain activity.

Speech-restructuring training changes connectivity within sensorimotor integration network

Reorganization of brain functions after short-term stuttering interventions have been reported for task-related[36,42] as well as spontaneous MRI signal fluctuations[35,36] in fMRI. Strikingly, such studies have reported increased activity of the left IFG, the basal ganglia or a decreased activity of the right hemisphere[36–38,40,42]. These structures however are part of different speech networks. For example, the left IFG attributes to speech motor planning as well as sensorimotor integration[59] whereas right hemispheric activity including the IFG could be part of the inhibition network[44] (Figure 1). We thus hypothesized that the intervention under study here could lead to an increased connectivity within the networks of speech motor planning, articulatory convergence or sensorimotor integration network or to a decreased connectivity within the motor inhibition network. Interestingly, connectivity increase was restricted to key functional brain hubs of sensorimotor integration and speech motor learning. Specifically, the observation of an increased rs-fMRI connectivity of the left IFG with the left LMC is new. While previous studies performed hypothesis-free whole-brain analyses, our ROI-to-ROI analysis was hypotheses-driven, and restricted to four semi-discrete networks that closely relate to the stuttering trait and to the behavioral changes that are targeted by the specific speech restructuring intervention. Other speech-related networks such as the network of speech planning, articulatory convergence or motor inhibition remained unchanged. Thus, the

intervention under study strengthened the interplay of the neurobiological substrate of sensorimotor integration required to learn a new speech technique.

Recovered fluent speech relates to a strengthened synchronization of the left IFG with the left laryngeal motor cortex and the right posterior superior temporal gyrus

The studied intervention encompassed one year of learning and practicing a new speech technique. This speech technique comprises soft voice onsets, consonant lenitions, and controlled sound prolongations[30]. Thus, voicing and timing are the key features under change over the course of the acquisition of the new speech technique. The control of voicing is based on the neural control of the larynx and involves the LMC[60–65], while the control of speech timing involves activity of the posterior part of the inferior frontal gyrus pars opercularis[44,66,67]. Accordingly, the intensive training incorporated two brain regions, the left LMC and the left IFG, that provide essential neural contributions to fluent speech production.

In the current study we found that the intervention strengthened connectivity between the left IFG and the left LMC. This finding is also consistent with the involvement of the left posterior IFG and left motor cortex in motor learning in general[68], and with the particular involvement of the posterior IFG and the left LMC in speech motor learning[6,69]. The IFG and the orofacial motor cortex share direct connections[70], and are commonly co-active under task- and resting-state conditions[61,71]. Theories on speech motor control assume the posterior region of the IFG to link the target speech unit to an articulatory code that is subsequently implemented by the motor cortices that finally orchestrate the articulators, including the larynx[9]. Hence, vital connectivity between the left IFG and left LMC is particularly important for the acquisition of speech or of a new speech technique.

Intervention also strengthened co-activity between the left IFG and the right pSTG. The speech motor system is required to monitor the auditory feedback signal, to rapidly correct small articulatory errors in natural speech. Speech-related auditory feedback control involves the right pSTG and task-related co-activations of the left posterior IFG with bilateral pSTGs[3,5,9,59,72]. The standard model of speech

motor control suggests that the posterior IFG provides feedforward control signals and the pSTG conveys feedback-based corrective signals[9]. Learning and practicing a new speech technique addresses neural circuitries of auditory feedback monitoring because patients are constantly required to adjust the sound of their speech to fit it to the new auditory target space. We suggest that the increased co-activity between left IFG and right pSTG could reflect the frequent recruitment of both brain regions and auditory feedback control mechanisms during learning and practicing the new speech technique.

Here, we measured MRI signal fluctuations in the absence of response demands or external stimulation to describe intervention-induced changes to the speech function-related sensorimotor integration network. It is assumed that spontaneous brain activity at rest relates to the underlying anatomical circuitry[73] as supported by diffusion weighted imaging[74,75]. Specifically, it has been suggested that spatially and temporally correlated brain activity at rest arises from neuronal noise between brain areas that share anatomical connections[73]. In this respect, the current study extends previous studies where task-related changes in brain activity were observed as a result of the very same intensive stuttering intervention[37,38,40,41]. However, task-related neuroimaging results from learning studies might be confounded by behavioral changes. Using resting-state activity as a neural marker of neuroplasticity rules out that changes in brain activity were induced by changes in task performance[6]. In fact, here we provide a purely neurophysiological index of neuroplasticity in the context of an intensive stuttering intervention.

In this study, rs-connectivity and behavioral changes did not correlate. Two other long-term intervention studies did not report any correlations between brain activity and behavioral change[37,42]. Correlations of brain activity with enhanced speech fluency in other stuttering intervention studies are based on direct measurements after intervention[35,36,40], task-based brain activity[36,40,41] or on cerebellar rs-connectivity[35]. The lack of seed regions in the cerebellum is one limitation of the current study. Previous studies reported the cerebellum to be a region of intervention-induced neural reorganization in stuttering[35,40,42], a finding that has not been replicated

in a more recent study[36]. Because in our study the field of view of the EPI sequence did not cover the whole brain, making it impossible to include ROIs of the cerebellum. In addition, correlational effects between connectivity strength and adherence to practice cannot be investigated as commitment to practice was not documented. Last, due to a limited acquisition time of two years, groups varied significantly in age. Age differences seem to have influenced reported changes in connectivity between left IFG and left SMG (please refer to the supplementary discussion).

No long-term changes of diffusion properties in major speech tracts

Here, long-term plasticity was evident in an increased synchronization of crucial left cortical speech motor regions. Related white matter tracks showed no plasticity in concert with fluency enhancement. Although, this is surprising, since for other domains such as reading intervention white matter changes have been reported[58], our findings agree with the only previous DTI investigation[40] on stuttering intervention. Still, brain-behavior relationships changed with changes in behavior. After therapy, stuttering severity was negatively correlated with FA in the left SLF such that the higher the FA values in the SLF the milder the stuttering after intervention. One possible interpretation could be that the strength of the SLF facilitates therapy outcome. Furthermore, after therapy, FA in the right FAT correlated positively with the psycho-social impact of stuttering, meaning the weaker the suffering from stuttering the lower the FA values in the right FAT. Strikingly, the right FAT is associated with action inhibition and it was recently hypothesized that hyperactive inhibitory circuits contribute to the occurrence of stuttered speech[26]. The current observation further suggests, that relieve from stuttering is associated with weaker connectivity of related inhibitory structures.

Perspectives with regard to other therapeutic approaches to ameliorate stuttering

Common stuttering interventions consist of (1) speech motor interventions partly modifying or fully reshaping laryngeal, articulatory or respiratory movements, (2) feedback and technology

interventions, which, e.g., use delayed auditory feedback to enhance fluency, or visual feedback to support speech motor interventions, (3) behavioural modification interventions, or (4) cognitive interventions improving psychological well-being, self-confidence, and self-conception. The current and previous studies tested neurofunctional correlates of brain reorganization for the first two approaches. The neurobiological foundation of an intervention-induced relief from stuttering due to the fourth approach, such as for example the cognitive-behaviour intervention[76], would be highly interesting and an essential complement. Of greatest importance are future studies with children with persistent stuttering to test whether reorganization induces neurotypical brain functioning and to develop therapeutic strategies that protect children from relapse.

Conclusion

A one-year practice of fluency-shaping speech techniques boosts the synchrony of spontaneous brain activity in core hubs of speech timing and voice control. Thus, successful speech restructuring shapes sensorimotor integration networks and is reflected in a long-lasting, focal, neurofunctional reorganization.

References

1. Andreatta, R. D., Stemple, J. C., Joshi, A. & Jiang, Y. Task-related differences in temporo-parietal cortical activation during human phonatory behaviors. *Neuroscience Letters* **484**, 51–55 (2010).
2. Price, C. J. A review and synthesis of the first 20 years of PET and fMRI studies of heard speech, spoken language and reading. *Neuroimage* **62**, 816–847 (2012).
3. Tourville, J. A., Reilly, K. J. & Guenther, F. H. Neural mechanisms underlying auditory feedback control of speech. *NeuroImage* **39**, 1429–1443 (2008).
4. Hickok, Houde, J. & Rong, F. Sensorimotor Integration in Speech Processing: Computational Basis and Neural Organization. *Neuron* **69**, 407–422 (2011).

5. Behroozmand, R. *et al*. Sensory-motor networks involved in speech production and motor control: an fMRI study. *Neuroimage* **109**, 418–428 (2015).
6. Darainy, M., Vahdat, S. & Ostry, D. J. Neural Basis of Sensorimotor Plasticity in Speech Motor Adaptation. *Cereb. Cortex* **29**, 2876–2889 (2019).
7. Turkeltaub, P. E., Eden, G. F., Jones, K. M. & Zeffiro, T. A. Meta-Analysis of the Functional Neuroanatomy of Single-Word Reading: Method and Validation. *NeuroImage* **16**, 765–780 (2002).
8. Brown, S., Ingham, R. J., Ingham, J. C., Laird, A. R. & Fox, P. T. Stuttered and fluent speech production: an ALE meta-analysis of functional neuroimaging studies. *Hum Brain Mapp* **25**, 105–117 (2005).
9. Guenther, F. H. *Neural Control of Speech*. (MIT Press, 2016).
10. Xue, G., Aron, A. R. & Poldrack, R. A. Common Neural Substrates for Inhibition of Spoken and Manual Responses. *Cereb Cortex* **18**, 1923–1932 (2008).
11. Ghahremani, A. *et al.* Stopping and slowing manual and spoken responses: Similar oscillatory signatures recorded from the subthalamic nucleus. *Brain Lang* **176**, 1–10 (2018).
12. Kraft, S. J. & Yairi, E. Genetic bases of stuttering: The State of the Art, 2011. *Folia Phoniatrica et Logopaedica* **64**, 34–47 (2012).
13. Büchel, C. & Sommer, M. What Causes Stuttering? *PLOS Biology* **2**, e46 (2004).
14. Chang, S.-E., Garnett, E. O., Etchell, A. & Chow, H. M. Functional and Neuroanatomical Bases of Developmental Stuttering: Current Insights: *The Neuroscientist* (2018) doi:10.1177/1073858418803594.
15. Etchell, A. C., Civier, O., Ballard, K. J. & Sowman, P. F. A systematic literature review of neuroimaging research on developmental stuttering between 1995 and 2016. *J Fluency Disord* (2017) doi:10.1016/j.jfludis.2017.03.007.
16. Budde, K. S., Barron, D. S. & Fox, P. T. Stuttering, induced fluency, and natural fluency: A hierarchical series of activation likelihood estimation meta-analyses. *Brain and Language* **139**, 99–107 (2014).

17. Belyk, M., Kraft, S. J. & Brown, S. Stuttering as a trait or state - an ALE meta-analysis of neuroimaging studies. *Eur. J. Neurosci.* **41**, 275–284 (2015).

18. Belyk, M., Kraft, S. J. & Brown, S. Stuttering as a trait or a state revisited: motor system involvement in persistent developmental stuttering. *Eur. J. Neurosci.* **45**, 622–624 (2017).

19. Neef, N. E., Anwander, A. & Friederici, A. D. The Neurobiological Grounding of Persistent Stuttering: from Structure to Function. *Curr Neurol Neurosci Rep* **15**, 63 (2015).

20. Sommer, M., Koch, M. A., Paulus, W., Weiller, C. & Büchel, C. Disconnection of speech-relevant brain areas in persistent developmental stuttering. *Lancet* **360**, 380–383 (2002).

21. Watkins, K. E., Smith, S. M., Davis, S. & Howell, P. Structural and functional abnormalities of the motor system in developmental stuttering. *Brain* **131**, 50–59 (2008).

22. Cykowski, M., Fox, P. T., Ingham, R. J., Ingham, J. C. & Robin, D. A. A study of the reproducibility and etiology of diffusion anisotropy differences in developmental stuttering: a potential role for impaired myelination. *NeuroImage* **52**, 1495–1504 (2010).

23. Cai, S. *et al.* Diffusion imaging of cerebral white matter in persons who stutter: evidence for network-level anomalies. *Frontiers in Human Neuroscience* **8**, (2014).

24. Connally, E. L., Ward, D., Howell, P. & Watkins, K. E. Disrupted white matter in language and motor tracts in developmental stuttering. *Brain and Language* **131**, 25–35 (2014).

25. Kronfeld-Duenias, V., Amir, O., Ezrati-Vinacour, R., Civier, O. & Ben-Shachar, M. Dorsal and ventral language pathways in persistent developmental stuttering. *Cortex* **81**, 79–92 (2016).

26. Neef, N. E. *et al.* Structural connectivity of right frontal hyperactive areas scales with stuttering severity. *Brain* **141**, 191–204 (2018).

27. Kronfeld-Duenias, V., Amir, O., Ezrati-Vinacour, R., Civier, O. & Ben-Shachar, M. The frontal aslant tract underlies speech fluency in persistent developmental stuttering. *Brain Struct Funct* **221**, 365–381 (2016).

28. Giraud, A.-L. *et al.* Severity of dysfluency correlates with basal ganglia activity in persistent developmental stuttering. *Brain and Language* **104**, 190–199 (2008).

29. Metzger, F. L. *et al.* Shifted dynamic interactions between subcortical nuclei and inferior frontal gyri during response preparation in persistent developmental stuttering. *Brain Struct Funct* 1–18 (2017) doi:10.1007/s00429-017-1476-1.

30. Euler, H. A., Gudenberg, A. W. v, Jung, K. & Neumann, K. Computergestützte Therapie bei Redeflussstörungen: Die langfristige Wirksamkeit der Kasseler Stottertherapie (KST). *Sprache · Stimme · Gehör* **33**, 193–202 (2009).

31. Calmels, C. Neural correlates of motor expertise: Extensive motor training and cortical changes. *Brain Res.* **1739**, 146323 (2020).

32. Vahdat, S., Darainy, M., Milner, T. E. & Ostry, D. J. Functionally Specific Changes in Resting-State SensorimotorNetworks after Motor Learning. *The Journal of Neuroscience* **31**, 16907–16915 (2011).

33. Deco, G., Jirsa, V. K. & McIntosh, A. R. Emerging concepts for the dynamical organization of resting-state activity in the brain. *Nat Rev Neurosci* **12**, 43–56 (2011).

34. Albert, N. B., Robertson, E. M. & Miall, C. R. The resting human brain and motor learning. *Current Biology* **19**, 1023–1027 (2009).

35. Lu, C. *et al.* Neural anomaly and reorganization in speakers who stutter: a short-term intervention study. *Neurology* **79**, 625–632 (2012).

36. Lu, C. *et al.* Reorganization of brain function after a short-term behavioral intervention for stuttering. *Brain and Language* **168**, 12–22 (2017).

37. Neumann, K. *et al.* The nature and treatment of stuttering as revealed by fMRI: a within- and between-group comparison. *Journal of Fluency Disorders* **28**, 381–410 (2003).

38. Neumann, K. *et al.* Cortical plasticity associated with stuttering therapy. *Journal of Fluency Disorders* **30**, 23–39 (2005).

39. Neumann, K. *et al.* The Pathogenesis, Assessment and Treatment of Speech Fluency Disorders. *Dtsch Arztebl Int* **114**, 383–390 (2017).

40. Kell, C. A. *et al.* How the brain repairs stuttering. *Brain* **132**, 2747–2760 (2009).

41. Kell, C. A., Neumann, K., Behrens, M., von Gudenberg, A. W. & Giraud, A.-L. Speaking-related changes in cortical functional connectivity associated with assisted and spontaneous recovery from developmental stuttering. *Journal of Fluency Disorders* (2017) doi:10.1016/j.jfludis.2017.02.001.

42. Toyomura, A., Fujii, T. & Kuriki, S. Effect of an 8-week practice of externally triggered speech on basal ganglia activity of stuttering and fluent speakers. *NeuroImage* **109**, 458–468 (2015).

43. Neumann, K. *et al.* Assisted and unassisted recession of functional anomalies associated with dysprosody in adults who stutter. *Journal of Fluency Disorders* **55**, 120–134 (2018).

44. Neef, N. E. *et al.* Left posterior-dorsal area 44 couples with parietal areas to promote speech fluency, while right area 44 activity promotes the stopping of motor responses. *NeuroImage* **142**, 628–644 (2016).

45. Deco, G. & Corbetta, M. The Dynamical Balance of the Brain at Rest. *Neuroscientist* **17**, 107–123 (2011).

46. Kronfeld-Duenias, V., Amir, O., Ezrati-Vinacour, R., Civier, O. & Ben-Shachar, M. Dorsal and ventral language pathways in persistent developmental stuttering. *Cortex* **81**, 79–92 (2016).

47. Primaßin, A. Longitudinal structural and functional brain changes associated with stuttering improvement by therapy or brain lesion. (Georg August University, 2019).

48. Oldfield, R. C. The assessment and analysis of handedness: the Edinburgh inventory. *Neuropsychologia* **9**, 97–113 (1971).

49. Riley, J., Riley, G. & Maguire, G. Subjective Screening of Stuttering severity, locus of control and avoidance: research edition. *Journal of Fluency Disorders* **29**, 51–62 (2004).

50. Yaruss, J. S. & Quesal, R. W. *OASES: Overall Assessment of the Speaker's Experience of Stuttering*. (Pearson Assessments, 2014).

51. Zhang, R., Geng, X. & Lee, T. M. C. Large-scale functional neural network correlates of response inhibition: an fMRI meta-analysis. *Brain Struct Funct* 1–18 (2017) doi:10.1007/s00429-017-1443-x.

52. Aron, A. R. & Poldrack, R. A. Cortical and Subcortical Contributions to Stop Signal Response Inhibition: Role of the Subthalamic Nucleus. *J. Neurosci.* **26**, 2424–2433 (2006).

53. Whitfield-Gabrieli, S. & Nieto-Castanon, A. Conn: a functional connectivity toolbox for correlated and anticorrelated brain networks. *Brain Connect* **2**, 125–141 (2012).

54. Goto, M. *et al.* Head Motion and Correction Methods in Resting-state Functional MRI. *Magn Reson Med Sci* **15**, 178–186 (2016).

55. Power, J. D., Barnes, K. A., Snyder, A. Z., Schlaggar, B. L. & Petersen, S. E. Spurious but systematic correlations in functional connectivity MRI networks arise from subject motion. *Neuroimage* **59**, 2142–2154 (2012).

56. Yeatman, J. D., Dougherty, R. F., Myall, N. J., Wandell, B. A. & Feldman, H. M. Tract profiles of white matter properties: automating fiber-tract quantification. *PLoS ONE* **7**, e49790 (2012).

57. Garyfallidis, E. *et al.* Dipy, a library for the analysis of diffusion MRI data. *Front Neuroinform* **8**, 8 (2014).

58. Huber, E., Donnelly, P. M., Rokem, A. & Yeatman, J. D. Rapid and widespread white matter plasticity during an intensive reading intervention. *Nature Communications* **9**, 2260 (2018).

59. Guenther, F. H., Ghosh, S. S. & Tourville, J. A. Neural modeling and imaging of the cortical interactions underlying syllable production. *Brain Lang* **96**, 280–301 (2006).

60. Brown, S., Ngan, E. & Liotti, M. A Larynx Area in the Human Motor Cortex. *Cereb Cortex* **18**, 837–845 (2008).

61. Simonyan, K., Ostuni, J., Ludlow, C. L. & Horwitz, B. Functional but not structural networks of the human laryngeal motor cortex show left hemispheric lateralization during syllable but not breathing production. *The Journal of Neuroscience* **29**, 14912–14923 (2009).

62. Rödel, R. M. W. *et al.* Human Cortical Motor Representation of the Larynx as Assessed by Transcranial Magnetic Stimulation (TMS). *The Laryngoscope* **114**, 918–922 (2004).

63. Olthoff, A., Baudewig, J., Kruse, E. & Dechent, P. Cortical Sensorimotor Control in Vocalization: A Functional Magnetic Resonance Imaging Study. *The Laryngoscope* **118**, 2091–2096 (2008).

64. Simonyan, K. The laryngeal motor cortex: its organization and connectivity. *Current Opinion in Neurobiology* **28**, 15–21 (2014).

65. Bouchard, K. E., Mesgarani, N., Johnson, K. & Chang, E. F. Functional organization of human sensorimotor cortex for speech articulation. *Nature* **495**, 327–332 (2013).

66. Long, M. A. *et al.* Functional Segregation of Cortical Regions Underlying Speech Timing and Articulation. *Neuron* **89**, 1187–1193 (2016).

67. Clos, M., Amunts, K., Laird, A. R., Fox, P. T. & Eickhoff, S. B. Tackling the multifunctional nature of Broca's region meta-analytically: Co-activation-based parcellation of area 44. *NeuroImage* **83**, 174–188 (2013).

68. Papitto, G., Friederici, A. D. & Zaccarella, E. The topographical organization of motor processing: An ALE meta-analysis on six action domains and the relevance of Broca's region. *NeuroImage* 116321 (2019) doi:10.1016/j.neuroimage.2019.116321.

69. Rauschecker, A. M., Pringle, A. & Watkins, K. E. Changes in neural activity associated with learning to articulate novel auditory pseudowords by covert repetition. *Hum. Brain Mapp.* **29**, 1231–1242 (2008).

70. Greenlee, J. D. W. *et al.* A Functional Connection Between Inferior Frontal Gyrus and Orofacial Motor Cortex in Human. *Journal of Neurophysiology* **92**, 1153–1164 (2004).

71. Simonyan, K. & Fuertinger, S. Speech networks at rest and in action: interactions between functional brain networks controlling speech production. *J. Neurophysiol.* **113**, 2967–2978 (2015).

72. Niziolek, C. A. & Guenther, F. H. Vowel Category Boundaries Enhance Cortical and Behavioral Responses to Speech Feedback Alterations. *J. Neurosci.* **33**, 12090–12098 (2013).

73. Deco, G. *et al.* Resting-State Functional Connectivity Emerges from Structurally and Dynamically Shaped Slow Linear Fluctuations. *J. Neurosci.* **33**, 11239–11252 (2013).

74. Honey, C. J. *et al.* Predicting human resting-state functional connectivity from structural connectivity. *PNAS* **106**, 2035–2040 (2009).

75. Hagmann, P. *et al.* Mapping the Structural Core of Human Cerebral Cortex. *PLOS Biology* **6**, e159 (2008).

76. Menzies, R., O'Brian, S., Lowe, R., Packman, A. & Onslow, M. International Phase II clinical trial of CBTPsych: A standalone Internet social anxiety treatment for adults who stutter. *J Fluency Disord* **48**, 35–43 (2016).

Acknowledgments

This work was supported by the DFG (SO 429/4-1 to M.S). We thank Bettina Helten for the co-analysis of the speech samples, Michael Bartl for supporting the organization of the behavioral data, and Britta Perl and Ilona Pfahlert for assistance with the acquisition of the MRI data.

Author contributions

AK, AP, PD, WP, MS, and NEN conceptualized and designed the study. AP acquired the data. AK and NEN analysed the rs-fMRI data. NEN analysed the dMRI data. AK and NEN interpreted the data, drafted, and revised the manuscript for content. NEN prepared figures. All authors reviewed the manuscript.

Additional Information

The author(s) declare no competing interests.